Volume 1, Number 2, 2008. pp. 79-87

Jordan Journal of Physics

ARTICLE

Magnitudes of Bremsstrahlung and Cyclotron Cooling From on-Axis Accretion Shocks onto AM-Her Systems

H. Y. Omari[a,b], M. H. Abu Kharma[c], H. Sabat[b] and M. M. Omari[d]

[a] *Department of Physics, Mu'tah University, Al-Karak, Jordan.*
[b] *Institute of Astrophysics and Space Sciences, AL-alBayt University, Mafraq, Jordan.*
[c] *Dept. of Basic Sciences, AL-Balga University, Amman, Jordan.*
[d] *Faculty of Hijjawi for Engineering Technology, Yarmouk University, Irbid, Jordan.*

Received on: 21/5/2008; Accepted on: 27/11/2008

Abstract: The article presents a calculation of relative phases and relative magnitudes for bremsstrahlung and cyclotron emissions from radiative accretion shocks onto binary Magnetic CVs (AM-Her systems). The calculation is carried out for a 0.3 solar mass white dwarf primary star, having a field $B_* = 30\,\mathrm{MG}$, and accretion rate of $L_{\mathrm{acc}} = 3.2\mathrm{x}10^{-3}\, L_{\mathrm{Edd}}$. Here L_{Edd} is the Eddington accretion luminosity. Individual on-axis accretion funnels are investigated corresponding to large radii at which field lines strike the equatorial plane ($a_0 \equiv r_{\mathrm{eq}}/R_* = 500, 300, 300, 200, 150, 100, \text{and } 80$). Results show a relatively low level cyclotron cooling, and thus permit decoupling.

Keywords: AM-Her systems; Accretion shocks; Oscillations; Cyclotron cooling; Decoupling.

Introduction

Magnetic CVs (AM-Her systems) are semi-detached binary systems consisting of a secondary normal late-type red dwarf companion donor; transfering matter to a compact strongly magnetic accreting white dwarf primary star [11,14,21,22,26,33,48]. For a thorough review of CVs, see [2,11,55,60]. The strong magnetic field of the primary usually synchronizes the white dwarf spin to the orbital period [30]. The magnetic white dwarf primary acts like a particle accelerator. Electrons and ions of the fully ionized plasma in the preshock region spiral out along individual magnetic field lines and accrete directly onto the magnetic white dwarf along narrow accretion funnels, where the strong magnetic field of the white dwarf (10-100 MG) does not allow the formation of an accretion disk [8,9,14,50]. Some of the AM-Her systems (or Polars) contain highly magnetic white dwarfs with field strengths of (6-240 MG) [55]. Up to the year 1999, more than 80% of the ~65 known polars were discovered in the ROSAT All-Sky Survey (RASS [54]), with typical count rates for 15th-19th optical magnitudes in the range of 0.2-2.5 counts s^{-1} [3]. The selection criteria of high X-ray count rate and strong optical emission lines resulted in the discovery of polars in the intermediate-to-high accretion rate regimes [52].

Among the many products of the Sloan Digital Sky Survey [51,62] will be thousands of new white dwarfs extending to fainter than 20th magnitude, and distances greater than 1 kpc.

At intermediate accretion rates (1gm cm^{-2} s^{-1}), a strong standoff (standing) shock is formed above the surface, and the shocked gas cools mainly by 10-30 keV

Corresponding Author: H. Y. Omari. **Email**: rashed@mutah.edu.jo.

bremsstrahlung emission [30,52]. The bulk of emission from the magnetic white dwarf primary is presumably produced in strong shocks, formed as the plasma merges onto the magnetic white dwarf, whose surface acts as lower boundary cold stationary wall for the shock region [1,49,61]. The supersonic freely falling plasma is decelerated near the white dwarf surface, in a strong shock which heats the plasma to x-ray temperatures. The plasma becomes subsonic, and is thereby driven to oscillate with a typical oscillation time-scale similar to the cooling time-scale of the shock-heated plasma. The formed shocks are observed to emit hard x-rays and strongly polarized cyclotron optical emission, both of which are modulated on the orbital period [11,49]. The orbital separation of the binaries is small, such that the radius of the normal star exceeds its Roche lobe, and thus loses mass through the inner lagrangian point to the compact magnetic white dwarf primary star [56]. These studies stimulated searches for fast photometric variabilities in accreting magnetic white dwarfs and led to the discovery of optical quasi-periodic-oscillations (QPOs); for example, in the AM-Herculis systems: V834 Cen, AN UMa, EF Eri , VV Pup and BL Hydri [19,20,23,27,28,59]. For steady gas accretion at a rate dM/dt onto a magnetic white dwarf star of mass M_* and radius R_*, the accretion luminosity is

$$L_{\text{acc}} = |\Phi g|(dM/dt) = (GM_*/R_*)(dM/dt) \qquad (1)$$

The magnitude of the gravitational potential of the magnetic white dwarf is $|\Phi \text{g}| \sim 10^{17}$ - 10^{18} erg g^{-1}. For the modest accretion rates, $dM/dt \sim 10^{14}$ - 10^{18} $gm\ s^{-1}$. The calculated luminosities are consistent with those observed.

Magnetic field calculations are based on the interpretation that polarized light is due to cyclotron emission [6,25]. In some systems, the field strength has been found from Zeeman spectroscopy. AM-Her has B_* = 13 MG [12,18,34,46,57,63] ST LMi has B_* = 19 MG [45], BL Hyi has B_* = 30 MG [58], and V834 Cen has B_* = 22 MG [4]. The isolated white dwarf PG 2329+267 has B_* = 23 MG [29]. For RX J0453.4-4213, the analysis of the phase dependent movement of the maxima for Cyclotron harmonics leads to a magnetic field strength in the accretion region of B_* = 36 MG [5]. Optical studies of AX J2315-592, indicates that the main contribution to optical flux during the bright phase is from optically thin cyclotron emission in a relatively low magnetic field, B_* < 17 MG [53]. The improved sample statistics and uniformity indicate that the distribution of magnetic white dwarfs has a broad peak in the range ~ 5 – 30 MG [44]. Cataclysmic variables (CVs) have strong magnetic fields, B_* ~ 10-100 MG [11,14]. A relatively large number of them have B_* ~ 20-40 MG, which is one of the reasons that motivate the choice of B_* = 30 MG for our calculations. However, few of the AM-Her systems contain highly magnetic white dwarfs with field strengths ~ 240 MG [55].

The centered dipole configuration is able to fit the spectra for some stars. However, some others require longitudinally offset dipoles or even quadrupoles to obtain satisfactory fits [47]. Also some like WD1953-011 have peculiar field structure consisting of a high-field region covering about 10 percent of the surface area of the star, superimposed on an underlying relatively weak dipolar field [24]. The structure and shape of the accretion region, and hence the magnetic field topology, are probably more complicated than typically assumed.

Physical Picture and Numerical Model

The model assumes that a fully-ionized solar-composition-plasma flows from the companion star to the primary magnetic white dwarf star. Plasma flows along presumably dipolar magnetic field lines [13]. Thus, the one-fluid, one-dimensional time - dependent hydrodynamic equations are solved for plasma constrained to flow along individual dipolar field lines:

The mass continuity, momentum and energy equations, and the equation of state are solved to generate the time-dependent temperature and density structure of the hot post-shock plasma for independently oscillating magnetically confined flux tubes:

Mass continuity: $\frac{\partial \rho}{\partial t} + \nabla.(\rho \mathbf{v}) = 0$ (2)

Momentum equation:

$$\rho(\frac{\partial}{\partial t} + \mathbf{v}.\nabla)\mathbf{v} = -\nabla P - \rho \nabla \Phi_g + \rho F_{rad} \quad (3)$$

Energy equation:

$$\frac{\partial \rho I}{\partial t} = -P\nabla.\mathbf{v} - \nabla.(\rho I \mathbf{v} + q_e) - \Lambda \quad (4)$$

Equation-of-state: $P = (\gamma - 1)\rho I$ (5)

where $\gamma = 5/3$ is the adiabatic index.

For a complete description of hydrodynamic equations, see, for example, a previous work for off-axis accretion [31].

The oscillating shock cools off. The electron volume loss rate is a sum of three contributions: The electron-ion and electron-electron bremsstrahlung, and the Compton cooling [16]:

The electron thermal conductive flux, q_e, is given by

$$q_e = -K(T)\nabla T_e \quad (6)$$

where the conductive coefficient is

$$K(T_e) = \frac{1.8x10^{-5} T_e^{5/2}}{\ln(1.11x10^{-5} \rho^{-1/2} T_e)} erg/cm.s.K \quad (7)$$

Equations (2) to (7) are solved together using a modified version of SOLASTAR, a semi-implicit Lagrangian numerical code which uses artificial viscosity to model strong flow discontinuities [10,13,42]. The code performs the hydrodynamic calculations based on the assumption that bremsstrahlung strongly dominates cyclotron cooling, and the latter is not capable of damping shock oscillations. However, for strong fields ~ 50 MG, the cyclotron cooling strongly stabilizes all modes of the shock harmonic oscillation [43], and its effect is even more profound for sufficiently low accretion rates [15,17]. So the calculations in this work aim at examining the effect of the cyclotron cooling on shocks stabilization for the specific field value, B_* = 30 MG, which is typical for most of the magnetic white dwarfs in binary systems.

The first step is to generate the time dependent hydrodynamic structures based on the assumption that bremsstrahlung strongly dominates cyclotron cooling. The second step is to use the generated time-dependent structures to solve the radiative transfer problem for the cyclotron emission. The cyclotron emission is determined through a solution of the time-independent, static radiation transport equation for a hot plasma in the limit of large Faraday rotation [36]:

$$\frac{dI_\pm}{d\tau_\pm} = I_\pm - S_\pm \quad (8)$$

A time-independent formulation for the cyclotron transfer can be used; where the bulk of the emission comes from within an optical depth $\tau_\pm = 1$ i.e., photons escape essentially unscattered. Here $\tau_\pm$ is the optical depth through the accretion funnel. Plus and minus signs stand for the ordinary and extraordinary modes, respectively. The intensities from uncoupled radiation modes are: Ordinary mode intensity I_+ and extraordinary mode intensity I_-. For a plasma in local thermodynamic equilibrium, the source function $S_\pm$ is given by the local value of the Planck function:

$$S_\pm = B(T_i, \nu) = \frac{h\nu^3/c^2}{\exp(\frac{h\nu}{k_B T_i}) - 1} \quad (9)$$

The Planck function is calculated for various frequencies and positions across successive layers of the accretion funnel. The *i*th layer of the funnel is characterized by an average temperature T_i.

The magnetic field is assumed to be dipolar, and its magnitude at position *r* is

$$\left. \begin{array}{l} B(r, R_*, a_0) = \\ B_0 \, (R_*/r)^3 \sqrt{[1 - 3\, r/(4a_0 R_*)]} \end{array} \right\} \quad (10)$$

Here R_* is the radius of the magnetic white dwarf star, B_0 is the magnitude of the field at the polar surface of the star, $a_0 \equiv r_{eq}/R_*$ is a geometrical factor that measures, in units of R_*, the radius r_{eq} at which field lines strike the equatorial plane [32]. Various values of r_{eq} are taken, since the cyclotron emission region is seen to extend over a large range in magnetic latitude [35].

At the surface of the accretion funnel, the solution to the radiative transfer equation gives the following expressions for intensities:

$$\left.\begin{aligned} I_{\pm}(0,\nu,\mu) = \sum_{i=1}^{n-1} B(T_i,\nu)[\exp(-\tau_{\mathrm{i}},_{\pm}/\mu) \\ -\exp(-\tau_{\mathrm{i+1}},_{\pm}/\mu)] \end{aligned}\right\} \quad (11)$$

The time-dependent surface intensity $I_{\pm}(0,\nu,\mu)$ is evaluated for a variety of both photon frequencies ν and direction cosines μ with respect to the magnetic axis.

The Robinson and Melrose formula for the opacity [40,41] is used to calculate the ordinary and extraordinary mode optical depths ($\tau_{\mathrm{i}},_{\pm}$) from the surface of the funnel to the exterior surface of the ith. layer.

Finally, a comparison of relative magnitudes and phases between bremsstrahlung and cyclotron coolings will tell if this is reasonably right, where only in the weak cyclotron case can one decouple the radiative transfer equation from the hydrodynamic equations. An approximate study of the F mode [7] indicates that bremsstrahlung luminosity and cyclotron emission were π out of phase. There is a difference in phase between the Fundamental (F) and first-overtone-mode (1O) we study. This is due to the fact that cyclotron emission arises primarily near the shock front, and so it depends strongly on the shock temperature. It is found that the phasing of the shock luminosity and shock temperature for the F and 1O modes are different [13]. Now we choose to study the 1O mode because it does not get dampened, and its period corresponds to the period of QPOs, that are suggested to be cyclotron emissions associated with the 1O oscillations [39].

Results and Discusion

This article considers calculations for relative phases and magnitudes between Bremsstrahlung and total cyclotron luminosities from accretion shocks onto a magnetic white dwarf binary star of 0.3 solar mass, for an accretion luminosity L_{acc} = 3.2x10^{-3} L_{Edd}. The field $B_* = 30\,\mathrm{MG}$ is chosen to see if the corresponding cyclotron cooling can stabilize modes of the shock harmonic oscillation. Calculations are performed for on-axis accretion shocks: $a_0 \equiv r_{eq}/R_* = 500, 300, 300, 200, 150, 100,$ and 80. The chosen mass of the primary magnetic white dwarf binary star, 0.3 solar mass, corresponds to parameter regime of the optical QPOs observed in the above mentioned systems. However, the determination of the mass of the accreting white dwarf in magnetic cataclysmic variables using RXTE data shows higher masses, $\geq 0.44 M_s$ [37]. Also the analysis of the X-ray spectra of two strongly magnetic cataclysmic variables, DP Leo and WW Hor; using XMM-Newton, gives an estimate mass greater than M_S in both systems [38].

Total cyclotron luminosities are obtained from integrating both modes spectral intensities $I_{\pm}(0,\nu,\mu)$ over frequencies and directions. Results are presented in Figs. 1-6. Relative values; Brems/Cyc.; are calculated based on the fact that the bulk of the optically thick cyclotron emission emerges only from the surface of the accretion column, from within an optial depth of unity, and the escape time is much greater than the oscillation period of the shock. Whereas the optically thin bremsstrahlung emission escapes from the entire volume of the narrow shock region, the shock structure: height, temperature and luminosities vary sinusoidally with the same oscillation period of the shock. For example; the model $a_0 = 100$ has a first overtone mode period $0.11\,s$, and an approximate average shock height of $4.45 x 10^7\, cm = 0.046\, R_*$. At the surface of the white dwarf, the accretion column covers fractional areas of $f \approx (W/2R_*)^2 \sim 10^{-5} - 10^{-3}$, where W is the half width of the funnel at surface of star.

Most likely, for the chosen $B_* = 30\,\mathrm{MG}$ field strength, the cyclotron cooling does not stabilize modes of the shock harmonic oscillation. Results for all chosen values of the geometrical factor, a_0, emphasize that bremsstrahlung cooling is remarkabley larger than cyclotron cooling. Their approximate relative values are presented in Figs. 1-6, and results are summarized in Table (1). The relative value; Brems./Cyc., decreases with decreasing a_0. Thus, the cyclotron emission is of relevance for smaller a_0. For the geometrical factor, $a_0 = 80$, the local minimum value for this ratio is ≈ 57 (Fig. 6).

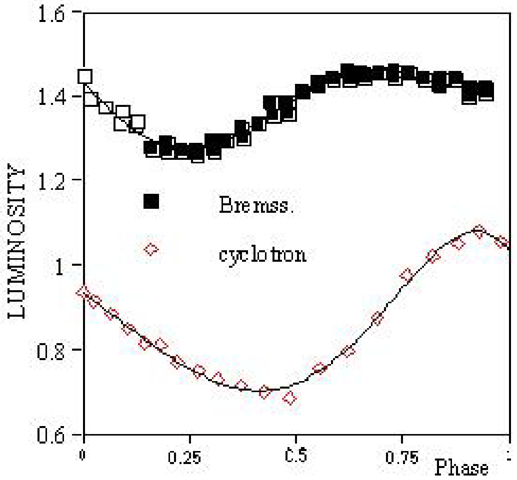

FIG.1. Relative phase between bremsstrahlung and total cyclotron luminosities for an accretion shock onto a white dwarf star of 0.3 solar mass, for an accretion rate L_{acc} = 3.2×10^{-3} L_{Edd}. Cyclotron luminosity is in units of 1.67 $\times 10^{30}$ erg/s, while bremsstrahlung luminosity is in units of 10^{32} erg/s. Bremsstrahlung is approximately 96 times greater than Cyclotron. Cyclotron leads bremsstrahlung by an approximate phase of 0.4π. Curves are for a_0 = 500.

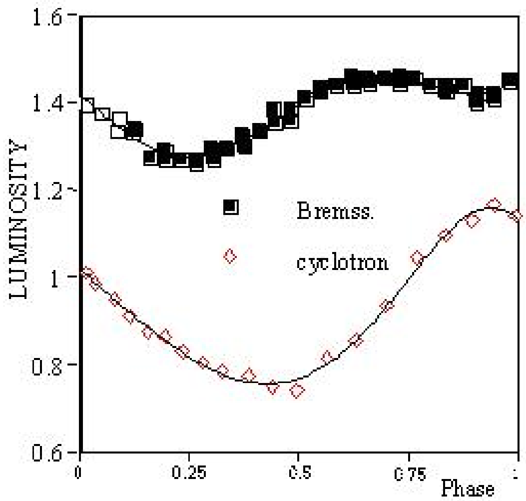

FIG.2. Relative phase between bremsstrahlung and total cyclotron luminosities for an accretion shock onto a white dwarf star of 0.3 solar mass, for an accretion rate *L*acc = 3.2x10-3 L_{Edd}. Cyclotron luminosity is in units of 1.67 x1030 erg/s, while bremsstrahlung luminosity is in units of 1032 erg/s. Bremsstrahlung is approximately 90 times greater than Cyclotron. Cyclotron leads bremsstrahlung by an approximate phase of 0.5π. Curves are for a_0 = 300.

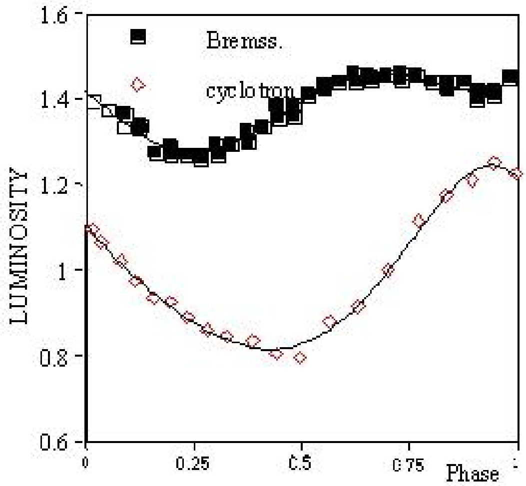

FIG.3. Relative phase between bremsstrahlung and total cyclotron luminosities for an accretion shock onto a white dwarf star of 0.3 solar mass, for an accretion rate *L*acc = 3.2x10-3 L_{Edd}. Cyclotron luminosity is in units of 1.67 x1030 erg/s, while bremsstrahlung luminosity is in units of 1032 erg/ s. Bremsstrahlung is approximately 82 times greater than Cyclotron. Cyclotron leads bremsstrahlung by an approximate phase of 0.55π. Curves are for a_0 = 200.

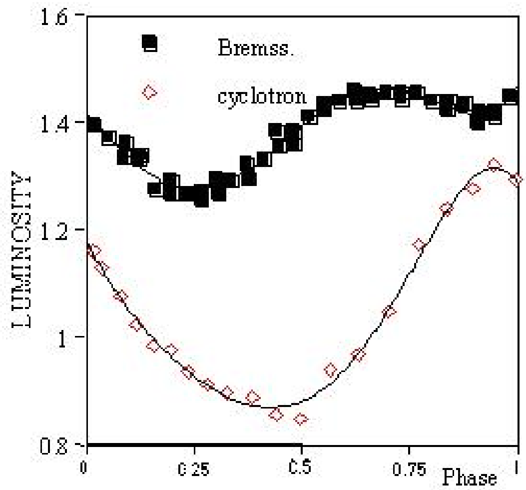

FIG.4. Relative phase between bremsstrahlung and total cyclotron luminosities for an accretion shock onto a white dwarf star of 0.3 solar mass, for an accretion rate L_{acc} = 3.2×10^{-3} L_{Edd}. Cyclotron luminosity is in units of 1.67 $\times 10^{30}$ erg/s, while bremsstrahlung luminosity is in units of 10^{32} erg/s. Bremsstrahlung is approximately 78 times greater than Cyclotron. Cyclotron leads bremsstrahlung by an approximate phase of 0.5π. Curves are for a_0 = 150.

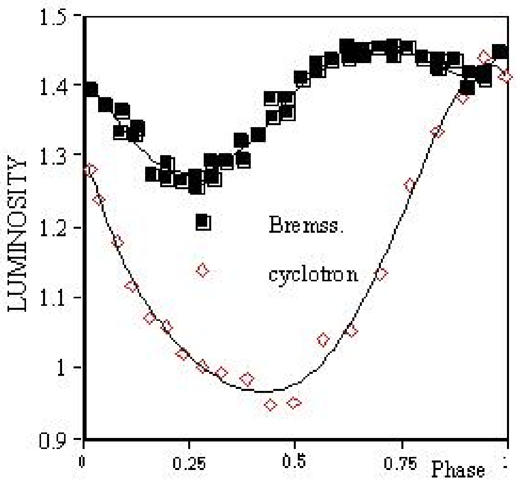

FIG.5. Relative phase between bremsstrahlung and total cyclotron luminosities for an accretion shock onto a white dwarf star of 0.3 solar mass, for an accretion rate *L*acc = 3.2x10-3 L_{Edd}. Cyclotron luminosity is in units of 1.67 x1030 erg/s, while bremsstrahlung luminosity is in units of 1032 erg/s. Bremsstrahlung is approximately 71 times greater than Cyclotron. Cyclotron leads bremsstrahlung by an approximate phase of 0.47π. Curves are for a_0 = 100.

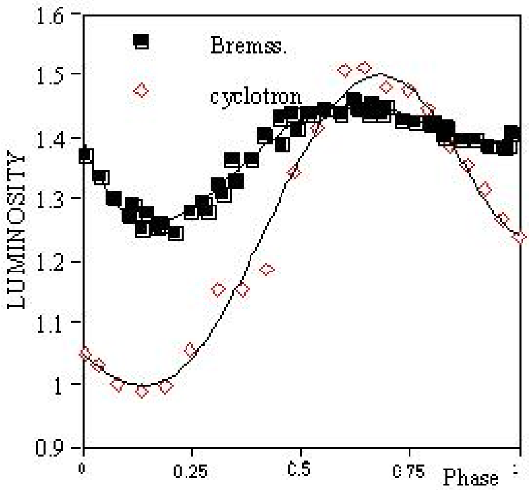

FIG.6. Relative phase between bremsstrahlung and total cyclotron luminosities for an accretion shock onto a white dwarf star of 0.3 solar mass, for an accretion rate L_{acc} = 3.2x10^{-3} L_{Edd}. Cyclotron luminosity is in units of 1.67 x10^{30} erg/s, while bremsstrahlung luminosity is in units of 10^{32} erg/s. Bremsstrahlung is approximately 65 times greater than Cyclotron. Cyclotron leads bremsstrahlung by an approximate phase of 0.12π. Curves are for a_0 = 80.

Thus the methodology of solving decoupled radiative hydrodynamic shock structure for the chosen parameters is justified for the 30MG field strength. Results predict a low level cyclotron cooling compared to bremsstrahlung, and thus one can decouple the radiative transfer problem from the hydrodynamic equations.

This work calculates time-dependent structures of radiative accretion shocks with a particular emphasis on the way in which they produce cyclotron optical emission. The study requires, in principle, the solution of the coupled multidimensional radiative hydrodynamic equations. Results show that even for B_* = 30 MG, the cyclotron is weak enough compared to bremsstrahlung. So no problem arises from decoupling the radiative transfer equation from the hydrodynamic equations, especially for on-axis accretion (i.e., the chosen large values of a_0). Thus, the time-dependent structure for the shocked plasma can be calculated without cyclotron cooling, and the resulting time-dependent structure is given to the radiative transfer code to calculate cyclotron intensities. This is legitimate for on-axis accretion on to the $0.3M_s$ primary star having B_* = 30 MG.

TABLE 1. Approximate relative values of bremsstrahlung cooling to cyclotron cooling, and the approximate phase angle ϕ that Cyclotron leads bremsstrahlung for various values of the geometrical factor a_0.

a_0	500	300	200	150	100	80
Brems./Cyc.	96	90	82	78	71	65
$\phi \cong$	0.4π	0.5π	0.55π	0.5π	0.47π	0.12π

Conclusion

Results for on-axis accretion ($a_0 \geq 80$), show that decoupling the radiative transfer equation from the hydrodynamic equations is justified for $B_* = 30\text{MG}$. Thus, results of calculations are correct for both hydrodynamic structures and cyclotron intensities, since the low level cyclotron cooling can not stabilize shock oscillations, and thus allows decoupling. Results are summarized in Table 1. They suggest that it is important to make the calculations for off-axis accretion, where cyclotron might turn out to be profound for $a_0 \cong 10$, in which case decoupling will not be safe.

References

[1] Aizu, K., Prog. Theor. Phys., 49 (1973) 1184.

[2] Beuermann, K., Radiation-hydrodynamic Models of the Accretion Spots in Magnetic Cataclysmic Variables, IAU Colloquium 190, 315 (2004) 187.

[3] Beuermann, K. and Burwitz, V. in ASP Conf. Ser. 85, Cape Workshop on Magnetic Cataclysmic Variables, ed. D. A. H. Buckley & B. Warner (San Francisco: ASP), (1995), p 99.

[4] Beuermann, K., Thomas, H.C. and Schwope, A. IAU Circ., No. 4775. V834 Centauri, (1989).

[5] Burwitz V., Reinsch K., Schwope A.D., Beuermann K., Thomas H.C-Greiner, Astron Astrophys, 305 (1996) 507.

[6] Chanmugam, G. and Dulk, G.A., ApJ, 244 (1981) 569.

[7] Chanmugam, G., Langer, S.H., and shaviv, G., ApJ, 299 (1985) 87.

[8] Chanmugam, G. and Wagner, R.L. ApJ, 213 (1977) L13.

[9] Chanmugam, G., and Wagner, R.L. ApJ, 222 (1978) 641.

[10] Cloutman, L.D. "Sola-Star: A One-Dimensional Iced-Ale Hydrodynamic Program For Spherically Symmetric Flows", Los Alamos Scientific Laboratory Report LA-8452-MS, (1980).

[11] Cropper, M.S., Space Science Rev., 54 (1990) 195.

[12] Hutchings, J.B., Crampton, D. and Cowley, A.P., ApJ, 247 (1981) 195.

[13] Imamura, J.N., Rashed, H.Y. and Wolff, M.T., ApJ, 378 (1991) 665.

[14] Katysheva, N.A. and Pavlenko, E.P., Astrophysics, 46 (2003) 114.

[15] King, A.R. and Lasota, J.P., MNRAS, 188 (1979) 653.

[16] Kylafis, N.D. and Lamb, D.Q., ApJ Supp. Ser. 48 (1982) 239.

[17] Lamb, D.Q. and Masters, A.R. ApJ, 234 (1979) L117.

[18] Latham, D.W., Liebert, J. and Steiner, J.E., ApJ, 246 (1981) 919.

[19] Larsson, S. Astr. Ap., 145 (1985) L1.

[20] Larsson, S. Astr. Ap., 181 (1987) L15.

[21] Liebert, J. and Stockman, H.S. in 7th North American Workshop on Cataclysmic Variables and Low Mass X-Ray Binaries, ed. D. Q. Lamb and J. Patterson (Dordrecht: Reidel), (1985) P151.

[22] Littlefair, S.P., Dhillon, V.S. and Martin, E.L., MNRAS, 340 (2003) 264.

[23] Mason, K.O., Middleditch, J., Cordova, F.A., Reichert, G., Murdin, P.G., Clarke, D. and Bowyer, S., ApJ, 264 (1983) 575.

[24] Maxted, P.F.L., Ferrario, L., Marsh, T.R. and Wickramasinghe, D.T., MNRAS, 315 (2000) L41.

[25] Meggitt, S.M.A. and Wickramasinghe, D.T., MNRAS, 198 (1982) 71.

[26] Mennickent, R.E. and Diaz, M.P., MNRAS, 336 (2002) 767.

[27] Middleditch, J., ApJ, 257 (1982) L71.

[28] Middleditch J., Imamura, J.N. and Steiman-Cameron, T.Y., ApJ, 489 (1997) 912.

[29] Moran, C., Marsh, T.R. and Dhillion, V.S., MNRAS, 299 (1998) 28.

[30] Mukai, K., Hellier, C., Madejski, G., Patterson, J., Skillman, D.R., ApJ, 597 (2003) 479.

[31] Omari, H.Y., Rabei, E.M. and Almulhem, A.A., Indian J. of radio and space phys. 31 (2002a) 7.

[32] Omari, H.Y., Almulhem, A. and Rabei, E., ABHATH AL-YARMOUK, Basic Sciences and Engineering, 11 (2002b) 287.

[33] Patterson, J., ApJ, 54 (1984) 443.

[34] Patterson, J. and Price, C., Publ. Astronm. Soc. Pacif., 93 (1981) 71.

[35] Potter, S.B., Cropper, M. and Hakala, P.J., MNRAS, 315 (2000) 423.

[36] Ramaty, R., ApJ, 158 (1969) 753.

[37] Ramsay, G., MNRAS, 314 (2000) 403.

[38] Ramsay, G., Cropper, M., Cordova, F., Mason, K., Much, R., Pandel, D. and Shirey, R., MNRAS, 326 (2001) L27.

[39] Rashed, H.Y., ApJ, 484 (1997) 341.

[40] Robinson, P.A., ApJ, 298 (1985) 161.

[41] Robinson, P.A. and Melrose, D.B., Aust. J. Phys. 37 (1984) 675.

[42] Ruppel, H.M. and Cloutman, L.D. "A General Numerical Fluid Dynamics Algorithm For Astrophysical Applications", Los Alamos Scientific Laboratory Report LA-6149-MS, (1975).

[43] Saxton, C.J., Wu, K. and Pongracic, H., Astronomical Society of Australia 14(2) (1997).

[44] Schmidt, G.D., Harris, H.C. Liebert, J., Eisenstein, D.J., Anderson, S.F., Brinkmann, J., Hall, P.B., Harvanek, M., Hawley, S., Kleinman, S.J., Knapp, G.R., Krzesinski, J., Lamb, D.Q., Long, D., Munn, J.A., Neilsen, E.H., Newman, P.R., Nitta, A., Schlegel, D.J., Schneider, D.P., Silvestri, N.M., Smith, J.A., Snedden, S.A., Szkody, P. and Berk, D.V., ApJ, 595 (2003) 1101.

[45] Schmidt, G.D., Stockman, H.S. and Grandi, S.A., ApJ, 271 (1983) 735.

[46] Schmidt, G.D., Stockman, H.S. and Margon, B., ApJ, 243 (1981) L157.

[47] Schmidt, G.D., West, S.C., Liebert, J., Green, R.F. and Stockman, H.S., ApJ, 309 (1986) 218.

[48] Smith, D.A. and Dihllon, V.S., MNRAS, 301 (1998) 767.

[49] Somova, N.N., Somova, T.A. and Najdenov, I.D., Astron. Astrophys. 332 (1998) 526.

[50] Stockman, H.S., Schmidt, G.D., Angel, J.R.P., Liebert, J., Tapia, S. and Beaver, E.A., ApJ, 217 (1977) 815.

[51] Stoughton, C., et al., AJ, 123 (2002) 485.

[52] Szkody, P., Anderson, S.F., Schmidt, G., Hall, P., Margon, B., Miceli, A., SubbaRao, M., Frith, J., Harris, H., Hawley, S., Lawton, B., Covarrubias, R., Covey, K., Fan, X., Murphy, T., Narayanan, V., Raymond, S., Rest, A., Strauss, M.A., Turner, E., Voges, W., Bauer, A., Brinkmann, J., Knapp, G.R. and Schneider, D.P., ApJ, 583 (2003) 902.

[53] Thomas H.C., Reinsch K., Astron. Astrophys., 315 (1996) L1.

[54] Voges, W., Aschenbach, B., Boller, Th., Bräuninger, H., Briel, U., Burkert, W., Dennerl, K., Englhauser, J., Gruber, R., Haberl, F., Hartner, G., Hasinger, G., Kürster, M., Pfeffermann, E., Pietsch, W., Predehl, P., Rosso, C., Schmitt, J.H.M.M., Trümper, J., Zimmermann, H.U., A&A, 349 (1999) 389.

[55] Warner, B. "Cataclysmic Variable Stars", (Cambridge univ. Press, Cambridge, 1995).

[56] Watson, C.A. and Dhillon, V.S., MNRAS, 326 (2001) 67.

[57] Wickramasinghe, D.T. and Martin, B., MNRAS, 212 (1985) 353.

[58] Wickramasinghe, D.T., Visvanathan, N. and Tuohy, I.R., ApJ, 286 (1984) 328.

[59] Wolff, M.T., Wood, K.S., Imamura, J.N., Middleditch, J. and Steiman-Cameron, T.Y., ApJ, 526 (1999) 435.

[60] Wu, K., Space Science Rev., 93 (2000) 611.

[61] Wu, K. and Cropper, M., MNRAS, 326 (2001) 686.

[62] York, D.G., et al., AJ, 120 (2000) 1579.

[63] Young, P., Schneider, D.P. and Shectman, S.A., ApJ, 245 (1981) 104.